Platypus: Sub-mm Micro-Displacement Sensing with Passive Millimeter-wave Tags As *"Phase Carriers"*

Thomas Horton King
Carnegie Mellon University
Pittsburgh, United States
thortonk@andrew.cmu.edu

Jizheng He
University of Illinois
Urbana-Champaign
Urbana, United States
jizheng4@illinois.edu

Chun-Kai Yao
University of Illinois
Urbana-Champaign
Urbana, United States
ckyao2@illinois.edu

Akarsh Prabhakara
Carnegie Mellon University
Pittsburgh, United States
akarsh@cmu.edu

Mohamad Alipour
University of Illinois
Urbana-Champaign
Urbana, United States
alipour@illinois.edu

Swarun Kumar
Carnegie Mellon University
Pittsburgh, United States
swaruk@cmu.edu

Anthony Rowe
Carnegie Mellon University
Pittsburgh, United States
agr@andrew.cmu.edu

Elahe Soltanaghai
University of Illinois
Urbana-Champaign
Urbana, United States
elahe@illinois.edu

ABSTRACT

Micro-displacement measurement is a crucial task in industrial systems such as structural health monitoring, where millimeter-level displacement of specific points on the structure or machinery displace can jeopardize the integrity of the structure and potentially leading to catastrophic damage or collapse. Traditionally, such displacements on large structures are measured using visual sensing platforms or advanced surveying equipment. However, they either fall short in varying weather and lighting conditions or require installation and maintenance of high-power sensing platforms that are expensive to deploy at scale, especially if continuous measurements are desired.

In this paper, we explore simultaneous tracking of quasi-static micro-displacements of multiple objects or multiple points from a single vantage point using millimeter-wave (mmWave) radars. We present Platypus, a micro-displacement sensing system that enables sub-millimeter level accuracy by using mmWave backscatter tags and their reflection as *phase carriers* to shift the phase changes due to tiny displacements to clean frequency bins for precise tracking. It then reconstructs the phase changes with sub-millimeter level accuracy even from extended ranges (over 100m) or in non-line-of-sight (NLoS) situations. While Platypus enables many different applications, we demonstrate the proof-of-concept in structural health monitoring, where mmWave tags are attached to building models and track the structural micro-displacements, achieving a median of 0.3 mm accuracy.

ACM Reference Format:
Thomas Horton King, Jizheng He, Chun-Kai Yao, Akarsh Prabhakara, Mohamad Alipour, Swarun Kumar, Anthony Rowe, and Elahe Soltanaghai. 2023. Platypus: Sub-mm Micro-Displacement Sensing with Passive Millimeter-wave Tags As *"Phase Carriers"*. In *The 22nd International Conference on Information Processing in Sensor Networks (IPSN '23), May 09–12, 2023, San*
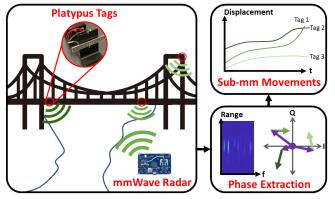
Figure 1: Platypus provides sub-mm multi-point micro-displacement sensing even at long ranges using passive mmWave backscatter tags as "carriers" of the phase.

Antonio, TX, USA. ACM, New York, NY, USA, 13 pages. https://doi.org/10.1145/3583120.3586965

1 INTRODUCTION

Measuring and tracking *micro-displacements* of multiple points in space from long ranges has important applications in several contexts ranging from structural health monitoring and environmental sensing to industrial robotics and automation. Consider, for example, structural health monitoring of bridges, where tracking of multiple points across the structure such as the bridge girder, tower, cables or around surface cracks helps detect internal defects that are often hidden before they can jeopardize the integrity of the structure. Despite the rich prior art in micro-displacement tracking, which use either traditional sensors (accelerometer, LVDT, RFID, etc), vision-based systems [34], or advanced surveying platforms [3], their limited accuracy or their prohibitive cost prevents them from being widely deployed in real application scenarios.

More recent solutions propose the use of radars for deflection detection [26] or vibration measurements [16] due to their resilience to obstruction, weather, and lighting conditions. The majority of these systems rely on phase measurements and phase changes across frames (samples) to calculate tiny displacements. These methods

have been even more effective with millimeter-wave (mmWave) radars, owing to their short wavelength and therefore higher sensitivity of phase changes. However, the performance of conventional phase reconstruction methods (e.g. [16]) drastically drops in dynamic environments with multiple moving objects with relatively similar speed and in close proximity of each other. In addition, such industrial and structural micro-displacements are often quasi-static – changing at millimeter level over long periods. Therefore, the phase changes caused by such displacements can be easily masked by the noise in the signal.

In this paper, we answer ***how to enable unstructured micro-displacement estimation using commodity mmWave radars?***. Similar to carrier waves in telecommunication that share wireless mediums via frequency division multiplexing, we demonstrate that by simply attaching passive modulating tags at the targets of interest, we can drastically improve the resolution and accuracy of micro-displacement measurements in dynamic environments. That is to say, we can use tag modulation frequencies as *phase carriers* to shift the phase changes due to the targets' micro-displacements apart from each other and other background reflectors.

This paper presents Platypus[1], a practical approach that provides multi-point micro-displacement measurement with sub-millimeter accuracy even at long ranges (up to 100 meters). Platypus achieves super-resolution tracking of displacements at a fraction of the wavelength at mmWave bands. Uniquely, we make no assumptions whatsoever on the trajectory or shape of this displacement, unlike prior work in vibration [16] or 1D displacement sensing [26]. Platypus builds on prior hardware realizations of mmWave backscatter tags [4, 5, 33], with key system design and new signal processing to enable sub-mm displacement tracking, in contrast to the centimeter-scale one-shot localization that prior work has achieved.

At a high level, Platypus operates on a familiar approach in backscatter tracking – it leverages the phase of wireless channels from tags to readers. However, unlike prior art on fine-grained RFID tracking [37, 39, 44], we mainly use the tags to shift the phase changes of each target to a different clean frequency bin to then reconstruct the micro-displacements of each tag. Specifically, the tags used by Platypus are designed to transmit repetitive square wave patterns of on-off keying at pre-designed rates, enabling a relatively simple hardware design. The square wave of the tag reflection signals in the time domain appears as a sinc function with harmonics at tag's modulation frequency in the frequency domain, which also carry the small phase changes due to micro-displacements. As such, closely located tags with similar velocities that could otherwise appear in the same range bin and Doppler frequency bins, will be separated into different modulation frequency bins by just selecting different modulation frequency rates for each tag.

While the use of mmWave tags allows us to deal with multipath and multi-point displacement tracking, it does not eliminate the phase noise induced by device circuits (e.g. oscillator or the mixer) or the wireless channel in low signal-to-noise ratios (SNRs). To address this challenge, we leverage a well-known signal leakage phenomenon caused by Discrete Fourier Transform (DFT) operations [15], that creates stretching of FFT peaks in neighboring

range bin. Unlike phase noise, the changes in the In-phase and Quadrature (IQ) domain due to tag displacements is constant across all these neighboring range bins. We exploit the inherent consistency among these signals to recover the tags' micro-displacement characteristics even in the presence of noise.

With the above two techniques, Platypus can accurately estimate the tag micro-displacement but only its projection along the line-of-sight direction of the tag reflection. To extract the micro-displacement vector including both the magnitude and direction, we propose a simple but effective triangulation algorithm between first-order and second-order reflections of the tag. More specifically, we place a passive synthetic reflector near the radar (within 1 m) to create a second-order reflection from the tag to the reflector and to the radar, which we then use to estimate the tag micro-displacement along another direction. The second-order and direct tag reflections create a triangle, which we further use to extract the displacement vector in 2D (and potentially 3D by placing more reflectors). The use of a synthetic reflector as opposed to another radar is cheaper and inherently handles phase synchronization and provides scalability for different industrial scenarios and applications with different accessibility hurdles (e.g. underneath a bridge, tall buildings, out-of-reach parts of the power plants, etc.). We envision Platypus's sub-millimeter, long-range and multi-point tracking capabilities enable many applications in industrial IoT such as structural health monitoring [10, 23, 26, 31] by allowing the monitoring of multiple points spanning the entire structure concurrently (Figure 1), with a radar mounted at a fixed point such as a support. The micro-displacements captured by the tags scattered at different points of interest can provide a holistic view of the stresses and displacement in the structure. These displacements, which can occur at sub-millimeter levels, can serve as an early detection mechanism for internal failures or excessive strain on the structure.

We prototype Platypus using off-the-shelf mmWave radars operating in 24GHz and custom designed state-of-the-art mmWave backscatter tags [4, 27, 33]. We evaluate our system in indoor and outdoor settings and show that accurate micro-displacement sensing (median accuracy of 0.3 mm) can be achieved without making any assumption about the displacement direction or path of movement even at long ranges (<100m). We demonstrate the robustness of Platypus in estimating pseudo-static micro-displacements at varied speeds, multipath scenarios, or even in NLoS scenarios where the tags are obstructed by different materials. As a proof of concept, we demonstrate the application of Platypus in structural health monitoring (SHM) for both lab-based and in-field testing.

Contributions: Our main contributions include:

- A novel design of a mmWave backscatter platform, as *carrier* of target micro-displacements, providing sub-millimeter accuracy from extended ranges.
- Platypus's algorithm and system design that obtains accurate and reliable signal phase measurements from tags stemming from minute displacements, despite ambient clutter and phase noises, obtaining micro-displacement vector (amplitude and direction) in 2D (and potentially 3D) space by leveraging a synthetic reflector.

---

[1]Platypuses are mammals whose electric field receptors are sensitive to tiny changes in electric field arising from prey that could be very far away.

- A detailed system implementation and evaluation in varied settings including a proof-of-concept evaluation of structural health monitoring using Platypus.

2 PRELIMINARIES

In this section, we first introduce the principles of displacement sensing using phase changes and why it can't be directly used for sub-mm micro-displacement measurements. We then describe the principles of backscatter sensing using mmWave tags and FMCW radars and how the tag can play an important role in precise micro-displacement measurements.

2.1 Phase-based Displacement Sensing

mmWave radars typically use frequency-modulated continuous wave (FMCW) chirps (pulses with linearly increasing frequency) as shown in Figure 2. To analyze the object reflections at the radar, the radar's received signal s_{IF} can be modeled as below after down-chirping and analog-to-digital conversions:

$$s_{IF;t}(n) = \sum_{k=1}^{K} \alpha_k \sin(\frac{4\pi B}{N c_0} R_k(t) n) \quad (1)$$

where n is the digital sample index, α is the amplitude of the received signal, K is the number of reflections, B is the chirp bandwidth of FMCW signal, N is the number of samples taken per chirp, c_0 is the speed of light, and $R(t)$ is the distance of the object and the radar at time t. As such, the intermediate frequency (IF) signal consisting of multiple tones can be processed using a Fourier Transform which results in the *Range-FFT Profile*, denoted as RP, with peaks at different range bins for each object. The movements of the objects create different phases at each chirp on the objects' corresponding range bin. In an ideal model (i.e free space, no hardware imperfection, and infinite sampling rate), we can simply extract the objects' micro-displacements by tracking the phase changes of the corresponding range bin across chirps: $\Delta x = \lambda \Delta \phi / 4\pi$.

However, in realistic models, the received signal in each range bin also includes the reflections from other objects in the same and nearby range bins. In addition, the received signal at the radar is significantly affected by noise such as the phase offsets through the mixing process and down-chirping. The combination of significant path loss in mmWave, high sensitivity of mmWave signals to noise, as well as tiny phase changes due to micro-displacements of small targets, makes this problem significantly more challenging. For example, conventional velocity measurement techniques use a sequence of N_c fast chirps collected in a 'frame' and perform a second-dimension FFT on RP (i.e. across the chirps) which results in the *Range-Doppler* grid, denoted as RD, with peaks at corresponding Doppler frequencies due to phase changes from movement. However, a slow pseudo-static micro-displacement creates a negligible Doppler frequency which is not detectable in commodity mmWave radars with limited sampling rate and buffer size (shown in Figure 2 as Obj 2).

2.2 Modeling mmWave Tag Reflection

Let us assume that a passive mmWave backscatter tag is attached to the target of interest with micro-displacements. The conventional mmWave tags in the literature [4, 27, 33] use *retro-reflective Van*
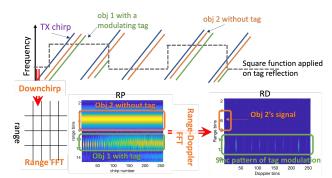

Figure 2: The tag's on-off-keying modulation appears as a sinc pattern in Range-Doppler profile, acting as a phase carrier, thus shifting tag micro-displacements to a clean frequency bin.
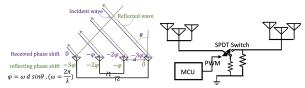

Figure 3: Typical structure of a mmWave tag using retro-reflective Van Atta arrays (left) and On-Off Keying modulation (right) at the tag.
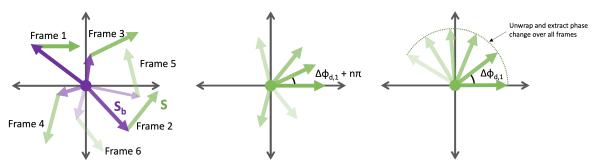
Atta antenna arrays [36] and some form of modulation (amplitude, frequency, or phase) to achieve long-range tag detection. Specifically, the tag consists of an array of antennas, connected in pairs, that passively reflect the incoming signals to the tag back along the exact same directions as the incidence, thus boosting the SNR of the tag reflected signal (shown in Figure 3). In addition, an RF switch is added to each transmission line between these antennas to create modulation by controlling the amount of reflections as it switches on and off, known as on-off-keying modulation. In favor of lower power consumption, Platypus adapts a simple circuitry at the tag by avoiding envelop detection circuitry or high-frequency oscillators and assumes that the tag is constantly modulating with no coordination between the tag and radar.

The on-off keying modulation of the tag appears as a square wave with the switching frequency of $f_{switch} = 1/T_{switch}$ applied on top of the tag reflection:

$$s_{IF;tag}(n) = \alpha \sin(\frac{4\pi B}{N c_0} R(t) n) \cdot \sum_{k=-\infty}^{\infty} sqr(\frac{2(nT_s - kT_{switch} - t_0)}{T_{switch}}) \quad (2)$$

where sqr(.) is a periodic square function, and T_s is the chirp sampling time corresponding to radar's chirp repetition frequency, and t_0 denotes the time offset between the start of the frame and the start of the square function (due to asynchronous tag-reader operations).

As the tag slowly moves due to the micro-displacements of the target, the Range-FFT Profile will have peaks at the same location with different phases across chirps. However, this phase still suffers from the noises due to other reflections with similar distances to the radar.

(a) Basic signal displacement model in the presence of background reflection and noise.

(b) Removing background reflections by shifting the displacement to a clean frequency.

(c) Unwrapping the phases of sequential frames to π to remove jumps from tag-read asynchronicity.

Figure 4: The signal models used in Platypus's stages.

Next, we calculate the Range-Doppler profile by performing a second-dimension FFT on RP. The square function of the tag modulations converts into a sinc function at range r_0 with the primary harmonic component equal to the tag's modulation frequency. As an intuitive representation, we compare the reflection pattern of two objects in Figure 2 in the Range-FFT and Range-Doppler profiles, Obj 1 is equipped with a tag and Obj 2 has no tag attached to it. We can see Obj 1's reflection at a clean frequency while Obj 2's reflection is embedded around Doppler-bin 0. Previous works [27, 33] use the sinc signature of the tag in Range-Doppler profile to perform absolute ranging on the tag reflection, but here we leverage it as a way to shift the target phase away from background interference and other objects at the same range. In the next section, we show why the phase changes due to the tag micro-displacements are now embedded into the harmonics of the sinc function and how the tag modulation frequency can be used as a "phase carrier" for precise phase reconstructions.

3 PLATYPUS DESIGN

3.1 Tag Modulation as "Phase Carrier"

A fundamental problem with phase-based micro-displacement is the signal noises due to background reflections at the same distance from the radar. Figure 4a shows this issue intuitively by showing the background reflections and noise as one composite reflection $\vec{S_B}$. This results in the asynchronous rotation of the micro-displacement signal, $\vec{S}$, across frames in the IQ domain. Previous solutions have addressed this issue by assuming a fixed motion pattern such as vibration [16, 38] or circular rotations [28, 45] as a model to fit the perceived phase changes to. However, Platypus makes no assumption about the displacement patterns or directions, which makes it even more challenging to extract tag phase changes in the time domain.

To address this problem, Platypus proposes a different approach: the use of a tag and its modulation to shift the phase changes due to the micro-displacements to a clean frequency bin in the Range-Doppler FFT (shown in Figure 4b). As mentioned in the previous section, the on-off switching of the tag appears as a sinc function in the Range-Doppler profile with a peak at the positive and negative modulation frequency bin, which also carries the phase changes of the tag reflection across frames. Note that a peak in the Range-Doppler FFT at a given range and frequency bin is essentially a

sine wave in the time domain, with the phase of the peak being the starting phase value of the sine wave. If the object representing this sine wave (in this case the tag) moves, the phase difference at the peak in Range-FFT profile between two frames will be equal to the amount of displacement.

However, the above algorithm only works if there is some form of synchronization across frames, such as the square wave that is applied on the tag reflection starts from the same time at all frames. Because we wish to conserve power to provide long-term micro-displacement monitoring, it is necessary to keep our tag asynchronous with the reader. This causes ambiguity in estimating the phase shift because a π phase shift from displacement (i.e negating the signal) would be equivalent to the tag square wave being sampled $T_s/2$ seconds later, and therefore phases in $[0, \pi)$ and $[\pi, 2\pi)$ alias such that $\phi \Leftrightarrow \phi + \pi$, where ϕ is the phase of the tag's reflection. However, assuming that the micro-displacements across frames are less than a quarter wavelength, we can eliminate this effect through phase unwrapping (shown in Figure 4c).

It should be noted that there are two underlying assumptions that make this approach work: (1) Since we are shifting the phase processing to the Range-Doppler FFT, we only get one sample for the entire frame (e.g. consisting of 64 chirps), much less frequently than Range-Profile-based methods. The elapsed time of a frame is around 10ms, and the displacements during this period are neglected. However, Platypus targets pseudo-static micro-displacements which change at a sub-millimeter level over long periods. Therefore, this assumption is held. (2) The modulation frequencies of the tags are selected carefully to avoid interference with other moving objects with a similar Doppler velocity. Given the maximum expected Doppler velocity of the moving objects in the tested environments, we can safely use modulation frequencies above $300Hz$.

3.2 Robust Micro-displacement Extraction

By shifting the micro-displacement signal to a clean frequency bin using the tag modulation frequency, we can eliminate the effect of the majority of background reflections in the same range bin. However, the extracted phase shifts at the tag's range bin still suffer from noise due to hardware imperfections and down-chirping. Given the sensitivity of phase values in mmWave bands and the low-SNR signals, even a small noise can completely mask the micro-displacement phase shifts. Previous works either ignore

(a) Range-Doppler (RD)　(b) Phase of RD across　(c) Magnitude of RD across　(d) I/Q across affected range
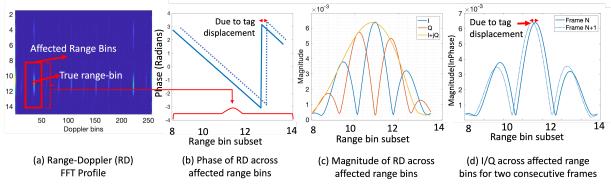FFT Profile　　　　affected range bins　　affected range bins　　bins for two consecutive frames

Figure 5: Platypus provides robust displacement extraction by tracking the phase changes across all affecting neighboring range-bins in I and Q domain.

these sources of noise, only achieving centimeter-level accuracy, or use chirp clustering for periodic, constrained displacements such as vibration [16]. However, none of these approaches are applicable for pseudo-static micro-displacement measurements. Our insight to address this issue is (1) IQ domain processing and (2) to exploit neighboring range-bins.

3.2.1 Phase-Shift Tracking in IQ Domain. In the Range-Profile signal, the real and imaginary signals modulate up and down with the tag. To eliminate the phase noises, Platypus pulls In-phase (real) and Quadrature (imaginary) components of the tag's modulation signal from the Range-Doppler FFT using the conjugate symmetry and linearity properties of FFTs:

$$f[n] = I(f[n]) + j \cdot Q(f[n]) \tag{3}$$

$$\{I(f[n]) \overset{FFT}{\Longleftrightarrow} F_I(\omega)\} \Longrightarrow \{F_I(\omega) = F_I(-\omega)^*\}$$
$$\{Q(f[n]) \overset{FFT}{\Longleftrightarrow} F_Q(\omega)\} \Longrightarrow \{F_Q(\omega) = -F_Q(-\omega)^*\} \tag{4}$$

Where $f[n]$ is an arbitrary function, $F(\omega)$ is an arbitrary FFT, $I(f[n])$ is the in-phase (real) component of $f[n]$, $Q(f[n])$ is the quadrature (imaginary) component of $f[n]$, and $*$ is the complex conjugation operator [30]. From these equations, we can extract the real and imaginary components of the tag's modulation by calculating the even and odd parts of the Range-Doppler FFT $RD(r, f)$. Knowing r_{tag} and f_{tag} from matched filtering [33], we can find the IQ components specifically at each tag signature's primary frequency, which will track with the phase change of the modulation's square wave.

$$I(f_{tag}) = \frac{RD(r_{tag}, f_{tag}) + RD(r_{tag}, -f_{tag})^*}{2}$$
$$Q(f_{tag}) = j \cdot \frac{RD(r_{tag}, f_{tag}) - RD(r_{tag}, -f_{tag})^*}{2} \tag{5}$$

$$\phi_{tag} = atan(\frac{I(f_{tag})}{Q(f_{tag})}) \tag{6}$$

$$\delta_n = \frac{\lambda}{4\pi} \cdot unwrap(\phi_n) \tag{7}$$

Where $I(f_{tag})$ and $Q(f_{tag})$ represent our estimate of the in-phase and quadrature magnitudes of the tag's modulation, *unwrap* reconstructs the modulation phase ϕ_{tag} by adding multiples of π,

and δ_n is the calculated radial displacement. Note that the phase of these measurements, i.e. where $I(f_{tag})$ and $Q(f_{tag})$ begin in *RP*, is implicitly used in Equation (6) for distinguishing if $I(f_{tag})$ and $Q(f_{tag})$ are in-phase or out-of-phase with each other.

3.2.2 Exploiting Neighboring Range Bins. In the above algorithm, if the I or Q component at a given range bin is small (i.e. ϕ approaches a multiple of $\pi/2$), that component can be dominated by noise and distorting the measured phase. To counter this, Platypus leverages a well-known phenomenon in FFT-based signal processing that the reflection of an object not only creates a peak at the true range bin in the Range-FFT Profile but also stretches to create a wide signature across multiple range bins. This is mainly due to the window effect in Discrete-Time Fourier Transforms, which creates side lobes around the frequency components [15]. Figure 5(a) shows this effect around the tag reflection in the Range-Doppler profile, stretching vertically along multiple range bins. The phase shift due to the tag micro-displacements will also appear at all of these range bins, in addition to a linear phase change across range bins due to the different underlying beat frequencies. Therefore, we can track the phase changes over all tag-affected range bins to provide more robustness to white or frequency-dependent noises.

Platypus finds the phase shift by autocorrelating the I and Q responses with simplified template signals of $|sin(\omega \cdot r + \phi)|$ and $|cos(\omega \cdot r + \phi)|$ respectively, for different ω, r, and ϕ values. The ϕ value with the highest correlation on both I and Q signals corresponds with the tag's phase shift. It should be noted that autocorrelating the I and Q signals are more resilient to noise due to the damped sine shape, with bins with low SNRs contributing the least to the autocorrelation (Figure 5(c)). This stretch also allows us to tell apart phases in $[0, \pi/2)$ and $[\pi/2, \pi)$ by distinguishing I/Q signals with positive and negative slopes (Figure 5(c)), information that was previously reconstructed from the more noise-prone measurement of the phase difference of I and Q.

3.2.3 Creating Synthetic Reflections. The phase reconstruction algorithm explained in the previous section effectively extracts the micro-displacements along the radial direction of the tag reflection. Therefore, if the tag is not moving perfectly toward or away from the radar, we only measure the projection of the tag displacement towards the LoS direction. In order to recover the micro-displacement vector, we need to estimate the displacements along two different known axes (or three axes for 3D tracking). Our initial
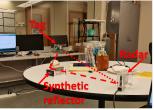
Figure 6: Using a synthetic reflector to extend Platypus's micro-displacement estimates to 2D (or 3D).
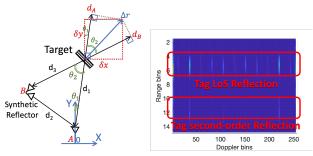

Figure 7: Extracting micro-displacement vector by combining the tag second-order and direct reflections.

system tried to accomplish this by looking at the displacements measured at different receiving antennas on the radar. However, the distance between the antennas is too small to create enough spatial diversity, especially in long ranges. In addition, the phases are too sensitive to noise for accurate micro-displacement measurement.

To address this challenge, Platypus leverages a synthetic reflection from a carefully placed reflector in the vicinity of the radar. The synthetic reflector, shown in Figure 6, consists of two high-gain antennas connected together with a wire, one antenna facing the radar and the other facing the tag. Therefore, it acts as a relay to redirect between the radar signal and the tag. Due to the tag's passive retro-reflectivity, the tag will reflect back each one of these paths toward its own direction. The received signal at the radar will include two dominant modulated reflections at two different range bins (due to length difference of the direct and the second-order reflections from the tag), shown in Figure 7. Platypus then performs the phase reconstruction for each reflection separately and calculates the micro-displacements along the direction of each path.

Our empirical studies show that the best synthetic reflector placement is within 1m distance from the radar. This not only ensures higher SNR for the tag's second-order reflection, but also ensures minimal overlap and interference between paths by offset the two reflections in range. To achieve this in practice, for each experiment, we tested locations within 1-2 m of the radar with the radar pointed directly at the reflector for the highest signal power. Since the targets of interest are assumed to be pseudo-static (e.g. stationary structures, or factory machinery), the synthetic reflector only needs to be deployed once for the entire duration of continuous monitoring.

3.3 Extracting Micro-displacement Vector

To convert the projected micro-displacements (d_A and d_B) to the true micro-displacement vector (Δr), Platypus forms a triangle as
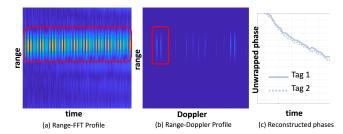

Figure 8: Platypus enables simultaneous tracking of multiple equi-range and equi-velocity points by using different tag modulation frequencies.

shown in Figure 7 between the two tag reflections that can be solved for δx and δy. First, using the conventional tag absolute range estimation described in Section 2.2, we can find d_1 and $d_2 + d_3$ (d_3, the distance from the radar to the synthetic reflector, is assumed to be measured during setup, so we can find d_2). θ_2, which demonstrates the angle between the two reflections from the tag, can be then calculated based on the law of cosines. In addition, θ_1 demonstrates the Angle-of-Arrival (AoA) of the tag direct reflection, which can be estimated using multiple antennas at the radar [33]. We use θ_1 to disambiguate which side of the LoS path the synthetic path is on, and to position multiple tags' displacements relative to each other in the 2D space. Because θ_1 has a larger uncertainty (due to our limited antenna count), we want our overall displacement magnitude to rely on θ_2, which is derived from the more accurate distance estimates. Note that we define the coordinate system with (0,0) at the radar location, and the positive y direction towards the 0-azimuthal direction of the radar. Finally, we define the unit vectors $\vec{u_A}$ and $\vec{u_B}$ in the two displacement directions A and B, and use a *Change of Basis* matrix to determine the micro-displacements in X and Y coordinate system using a simple matrix equation:

$$\begin{bmatrix} d_A \\ d_B \end{bmatrix} = \begin{bmatrix} comp_{\vec{u_A}}(\vec{r}) \\ comp_{\vec{u_B}}(\vec{r}) \end{bmatrix} = \begin{bmatrix} sin(\theta_1) & sin(\theta_1+\theta_2) \\ cos(\theta_1) & cos(\theta_1+\theta_2) \end{bmatrix} \cdot \begin{bmatrix} \delta x \\ \delta y \end{bmatrix} \quad (8)$$

$$\begin{bmatrix} \delta x \\ \delta y \end{bmatrix} = \begin{bmatrix} sin(\theta_1) & sin(\theta_1+\theta_2) \\ cos(\theta_1) & cos(\theta_1+\theta_2) \end{bmatrix}^{-1} \cdot \begin{bmatrix} d_A \\ d_B \end{bmatrix} \quad (9)$$

Where d_A and d_B are the two displacement magnitudes calculated in phase reconstruction steps, $comp_{\vec{u_A}}(\vec{r})$ is the projection of $\vec{r}$ onto $\vec{u_A}$, $\vec{u_A}$ is the unit vector of the displacement direction A, and δx denote the micro-displacements toward a standardized X direction. While θ_1 is used in Equation (9), it mainly impacts the direction of the displacement vector, not the overall magnitude of the displacement. Note that Platypus can be extended to 3D by using another synthetic reflector at a different location.

It should be noted that the Equation (9) will be invertible for a non-zero θ_2 between the synthetic reflection and the main LoS path. In addition, for very small angles between the two paths, the output displacements are expected to be much more sensitive and prone to errors, i.e. the transform matrix will be ill-conditioned. Thus, in addition to the constraints discussed in Section 3.2.3, the distance between the reflector and the radar should be set to achieve a sufficiently large angle between the two paths (e.g. at least 3°).

(a) 1D Prototype   (b) 2D Prototype

Figure 9: Platypus's tag prototypes.

Figure 10: Experimental setup both indoors and outdoors.

3.4 Scaling to Multi-point Tracking

In many applications (e.g. structural health monitoring, robotics, etc), there are typically multiple co-located components for which their relative displacements are even more important than the absolute displacement of each part. Therefore, it is essential to extend Platypus to simultaneous tracking of multiple operating tags that are co-located, essentially falling in the same range bin, and may even have very similar velocities. This use case is often ignored in RFID tracking due to lack of concurrent operation built into RFID EPC Gen2 protocol. However, Platypus can effectively provide this capability by deploying tags with different modulation frequencies, essentially separating the micro-displacements of different parts of the structure by shifting them to different frequency bins. As discussed in [33], approximately 30 tags with different modulation frequencies could be deployed in the same range bin with no overlap in the Range-Doppler FFT. The key intuition is that even if two tags fall in the same range bin in the time domain, their frequency-domain representation after the second FFT and the first harmonic of tag modulations will fall in two different frequency bins, allowing Platypus's phase reconstruction approach to work seamlessly. This allows us to additionally separate each tag's reflection from other tags within or outside of each tag's range bin.

Figure 8 demonstrates this effect in an intuitive manner by having two collocated tags modulating in 600Hz and 800Hz and moving on a motion stage at the same speed of 1mm/s toward the radar. We can see that even though the modulation pattern of the two signals are interleaved across chirps in the Range-FFT output (time domain), they appear in different frequency bins in the Range-Doppler profile due to their distinguished modulation frequencies. Platypus can then reconstruct the phase of each tag individually and track their displacements over frames. We evaluate and analyze this further in the next section, with co-located tags moving in separate directions.

4 IMPLEMENTATION

We implemented Platypus using a commercial mmWave radar, Analog Devices TinyRad [2], operating at $24GHz$ with $250MHz$ of bandwidth and $8dBm$ maximum power output. The radar integrates 4 on-board receiving and 2 transmitting antennas, but one TX antenna is used for the presented results in favor of lower latency. Multiple RX antennas are used for estimating AoA direction for tag reflections. The received signal is sampled at 1MHz and captured using MATLAB, directly polling data from the board. It should be noted that our choice of 24GHz was mainly due to the abundance of ultra-low-power electronics such as RF switches at the tag, but Platypus can be seamlessly extended to other bands in mmWave frequencies such as 77GHz.
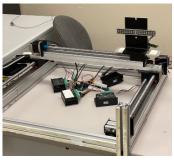
4.1 Platypus Tag Prototype

Inspired by recent developments [27, 29, 33] in retro-reflective mmWave tag designs for long-range operations, we develop a prototype of Platypus's tag using the tags proposed in [33]. The design uses ADRF5027 [1] RF switch evaluation kit and two off-the-shelf microstrip patch antennas each in a 2x8 array connected to the switch with short but matched length cables, creating a 2-element Van Atta array for retro-reflective behavior (shown in Figure 9). The tag is switching between retro-reflection, by letting the signal go through the transmission lines between the two antennas, and no-reflection, by terminating each of the antennas with a 50Ω to ground. This creates a simple on-off keying modulation that is used by the radar signal processing for detecting the tags and reconstructing their corresponding phase changes. For experiments with a synthetic reflector that require a wide AoA, we construct a 2D antenna array at the tag, shown in Figure 9(b), to create a larger field of view for tag detection from multiple angles.
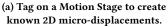
4.1.1 **Power Consumption**. While reducing the tag power consumption is not the main goal of this study, Platypus uses state-of-the-art mmWave tag designs with ultra low-power consumption [4, 33]. For majority of experiments, we use a constant modulation at 600-1100 switching per second, which corresponds to $2.6 - 2.71uW$ of power consumption and a corresponding continuous operation for 24 to 20.1 years, by using a 3V CR2032 lithium coin cell (235 mAh) with an efficiency of 75% and no battery self discharge. Alternatively, this amount of power can easily be harvested in outdoor use cases using small solar panels at the tag.
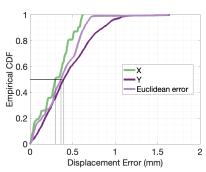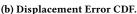
5 EVALUATION

We deploy our system in multiple indoor and outdoor environments, shown in Figure 10, including office buildings with rich multipath propagation due to the presence of furniture, metallic shelves, and long corridors, covered and open-space parking lots, and a structural engineering lab with different structural specimens made of concrete and steel with large metallic machinery in the background (shown in Figure 18). The tags are placed between 3m to 100m from the radar. For the benchmarking purposes, we used 1D and 2D linear motion stages, with 0.01mm resolution, to create different displacement vectors with different magnitude and in different directions at varying speeds, for a total of 100 experiments. The magnitude of generated displacements are between 1mm to 50cm (maximum length of the motion stage).
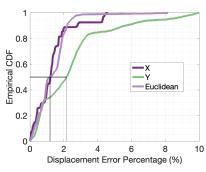
Ground Truth: For the experiments conducted with the motion stage, we used the generated motion vectors at the translation stage as the ground truth. We implemented a synchronization mechanism between the data collection laptop connected to the radar and the

(a) Tag on a Motion Stage to create known 2D micro-displacements.
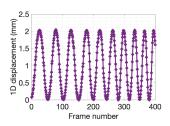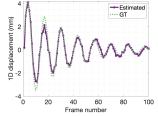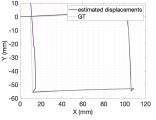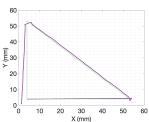
(b) Displacement Error CDF.

(c) Displacement Error % CDF.

Figure 11: Platypus achieves sub-mm accuracy with 2% median error percentage in estimating the 2D displacements across a wide range of experiments at different environments generated with a 2D motion stage.

(a) Sinusoidal Displacement

(b) Damped Sine Displacement

(c) Rectangular Displacement

(d) Triangular Displacement

Figure 12: Sample displacements estimated by Platypus.

computer that controls the motion stage. To synchronize the two systems, we initiate the motion from the data collection laptop by creating a socket between the two laptops. The duration of data collection is defined such that there are a few radar frames with no motion at the beginning and end of each command to the motion stage. This way, we can mark the start and end of each experiment and use the radar frame rate and displacement duration at the motion stage to create per frame ground truth. For experiments conducted in the structural lab, we used a high-precision Certus Opto-track system with active markers co-located with the mmWave tags as the ground truth for our experiments.

Baseline: To the best of our knowledge, Platypus is the first displacement sensing algorithm that can provide sub-mm accuracy even at long ranges. The closest available systems to Platypus are Tagoram [45] and RF-IDraw [41], which use off-the-shelf RFID tags and can achieve mm and cm level accuracy in tracking tag movements, respectively. However, Tagoram requires the tag's track function and RF-IDraw requires a large spacing in the reader's antenna array to disambiguate the phase measurements. In addition, both of these methods only work at short ranges below 10m. So, they would both be severely handicapped if run on setups designed for Platypus. Therefore, a head-to-head comparison would not be meaningful. However, for sensitivity analysis, we demonstrate the effectiveness of tag in separate the micro-displacement signal by comparing the results with a corner reflector as the baseline.

5.1 In-situ Micro-displacement Errors

We evaluate the performance of Platypus in estimating the displacement vector across all the experiments, both indoors and outdoors

at varying distances from the radar (2 m to 100 m). For ease of interpretation, we convert the displacement vector to displacements along X and Y axes defined relative to the norms of the radar. As shown in Figure 11(b), the median displacement error along X and Y axes are 0.36mm with 90th percentile of 0.6mm and 0.7mm along X and Y axes, respectively. Please note that the median error in these plots is higher than the 1D sensitivity analysis in the next Section, which is mainly caused by the micro-displacement vector extraction module. While Platypus is capable of measuring the micro-displacements with high accuracy, the absolute range estimates and AoA estimates are still bounded by the FFT accuracy, causing cm-level error in absolute range and 2-4 degree error in AoAs. These larger errors manifest in the multipath triangulation, which causes higher error along X and Y axes. It should be noted that the experiments contain a wide range of displacements from 1mm to 50cm at varying environments and multipath conditions, so the presented errors are considered the worst-case scenario results. We also measure the percentage of displacement error relative to the total displacement in each experiment point. As shown in Figure 11(c), Platypus provides a median of 2% percentage error (error compared to the total displacement) across experiments with 90th percentile of 6% in euclidean displacement estimates.

In addition, Platypus measures displacements per frame without making any assumption about the track of displacements. To demonstrate the capabilities of Platypus in estimating different shapes of motion, we imitate a few 2D displacements typically seen in industrial setups and structural displacements with a 2D motion stage, including a sine wave emulating friction-less harmonic
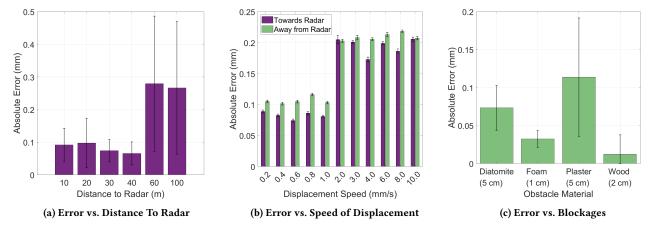
(a) Error vs. Distance To Radar   **(b) Error vs. Speed of Displacement**   **(c) Error vs. Blockages**

Figure 13: Platypus maintains sub-mm micro-displacement accuracy at varying ranges, displacement speeds, and NLoS scenarios.

motion (Figure 12(a)), a damped sine wave emulating damped oscillations (Figure 12(b)), and mm-scale triangular and rectangular displacements emulating movements of mechanical parts in industrial machinery (Figure 12(c) and (d)). We can see minor errors in estimated displacements at points with a sudden changes in displacement direction, which mainly happens when the change falls between two sequential frames. To improve the performance in these corner cases, we can increase the frame rate by decreasing chirps per frame. This trades higher accuracy with a reduction in the Doppler resolution (fewer distinguishable of tag frequencies). However, these two requirements rarely conflict in real scenarios, which prioritize (a) faster tracking or (b) wider Field-of-View (FoV).

5.2 Impact of Distance

Next, we evaluate Platypus's performance as a function of distance. We perform multiple experiments at each distance while keeping the environment and waveform parameters fixed across different trials (chirp duration of 500*us* and tag modulation frequency of 200kHz). Figure 13(a) shows the displacement accuracy of Platypus across different distances and we can see that it can maintain its sub-mm median accuracy at different ranges. At longer distances we see an increase in the error, which is due to significant attenuation of the tag reflections. It should be noted that the tag detection rate also decreases at longer ranges, dropping from 100% tag detection at ranges below 40m to 60% detection rate at 100m. Therefore, there are fewer samples in the longer range measurements, increasing uncertainty. To address these problems for longer distances, a larger Van Atta array or higher gain antennas can be used at the tag to increase the retro-reflectivity. Previous studies have shown that doubling the tag's antenna size from 2-element to 4-element can increase the gain by 80% [33].

5.3 Impact of Displacement Speed

To evaluate Platypus performance at different displacement speeds, we place the tag on a 1D motion stage and create forward and backward movements (toward or away from the radar) at varying speeds between 0.2mm/s to 10mm/s. The tag was placed 20m away, with *10mm of displacement for velocities below 1.0 mm/s and 100mm of displacement for velocities above 1.0 mm/s*. Figure 13(b)
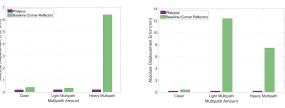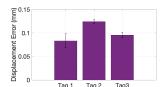

Figure 14: Impact of multipath in (left) different range bins and (right) the same range bin as Platypus's tag.

Figure 15: We stress test Platypus in severe multipath conditions by putting the tag in a rebar cage and a in front of a corner reflector.

shows that the average error is slightly higher at higher speeds but the maximum error is still less then 0.25mm. Compared to 0.3mm median accuracy in large-scale experiments, we can conclude that displacement speed does not have a significant impact in accuracy. The lower maximum error in these experiments is due to the shorter tag-to-radar ranges. Theoretically, we don't expect significant impact from displacement speeds as long as the amount of displacement between frames induces lower than $\frac{\pi}{2}$ change in phase (or π in complex radars). In addition, since Platypus estimates the displacement vector per frame, for higher speed displacements, reducing number of chirps per frame can improve response time. It should be noted that the pseudo-static micro-displacements are creating tiny displacements over long time, so the Doppler effect on tag movement is minimal and can be ignored.
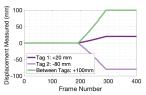
Figure 16: Platypus leverages the distinguished harmonics of tags modulation frequencies for phase reconstruction of three co-located tags.

5.4 Non-Line-of-Sight Performance

Next, we study Platypus's performance in Non Line of Sight (NLoS) scenarios. It is well-known that mmWave signals significantly attenuate by certain obstructions such as metal or human body, but we expect to detect the tag through other kinds of obstruction such as drywall, plaster, or concrete, which are common materials in industrial setups. We, therefore, evaluate the penetration capabilities of Platypus by placing the tag at different ranges from the reader between 10m to 35m and placing a large sheet of different materials to block the tag to reader view. We also make sure that the sheet blocks both LoS and potential multipath reflections from the tag by placing the sheet very close to the tag antennas. Figure 13(c) demonstrates the mean displacement errors in different NLoS scenarios and we can see that the tag is still detectable and maintains its sub-mm performance. This is significantly important in industrial plants and outdoor contexts such as construction sites or city structures, where optical displacement sensors fall short. In addition, in harsh industrial environments, Platypus tags can be easily protected by keeping in weatherized enclosures, thus providing an industrial-grade sensing solution. It should be noted that metal obstacles are only problematic if they block the tag reflections, but Platypusis robust to background reflections from metal or moving targets, which is tested in the next experiment.

5.5 Multipath Effect

While the majority of our experiments are conducted in office spaces with surrounding furniture and metallic shelves, acting as multipath reflectors, we specifically perform a more rigorous test for multipath sensitivity analysis. We interrogate a tag 10 m away, with no extra multipath in clean scenarios, 1 metal plate in light scenarios, and a metal plate and a moving person for the heavy scenarios. We also compare the results these experiment with the baseline that has a corner reflector as opposed to the tag. The results in Figure 14 show that Platypus's performance slightly degrades in the presence heavy multipath, but still preserves the sub-mm accuracy. However, it significantly outperform the corner reflectors. In addition, the max error i less than 0.15mm which is in line with Platypus's performance in shorter range and 1D micro-displacements.

We also stress tested Platypus in severe multipath conditions, (1) where the tag was placed in a rebar cage emulating a dense rebar arrangement inside concrete structures; (2) a corner reflector behind the tag, both shown in Figure 15. While the rebar cage is assumed to work like a Faraday cage for electromagnetic signals, we see negligible effect in tag detection and micro-displacement measurements. This is mainly because Platypus uses the tag's modulation frequency component to reconstruct the tag phase, while other metallic objects even in the same range bin, fall in different
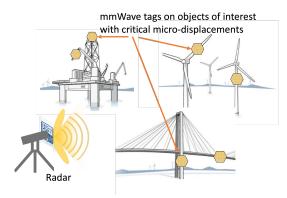

Figure 17: Platypus sub-mm micro-displacement performance at long range can enable new applications in structural health monitoring for monitoring of critical infrastructure such as bridges, power plants, tunnels, railroads, etc.

frequency bins. Even in cases with a moving metallic object nearby, the Doppler frequency due to the object movement will be much smaller than the Doppler frequency due to the tag modulation.

5.6 Multi-tag Performance

Platypus leverages the frequency multiplexing techniques [33] for multi-tag scenarios, in which each tag performs On-Off Keying at different rates. Theoretical analysis has shown Platypus's ability to support 25 to 100 simultaneous co-located tags[33], which is sufficient for our purpose. However, to evaluate the performance of Platypus in reconstructing the phase shift of multiple tags, we stress tested our system by placing two tags on top of each other and selecting two similar modulation frequencies of 650 Hz and 800 Hz. This causes the two tag reflections to interleave in both time and frequency domains. We applied different micro-displacements on both tags and compared the results with one tag only and when having two modulating tags at different range bins. As shown in Figure 16, we can successfully reconstruct each tag's phase shift and accurately track their displacements. This is mainly due to Platypus's phase reconstruction approach that relies on the harmonics of the tag's modulation frequencies. Therefore, the resolution of Platypus's micro-displacement sensing only depends on the spacing of the Doppler harmonics across Doppler frequency bins and will not be affected by how closely the two tags are located with respect to each other. This provides significant improvement over tagless tracking approaches [16] that purely rely on reflections from the object surface and therefore their displacement resolutions are limited by the range-bin resolution and the number of antennas at the radar.

6 PROOF-OF-CONCEPT APPLICATION: STRUCTURAL HEALTH MONITORING

In collaboration with the Civil and Environmental Engineering Department in our university, this section demonstrates a proof of concept application of Platypus in building displacement monitoring. Response of a structure under loads is a function of structural properties such as geometrical, material, and boundary conditions affecting the stiffness of the system and changes in the observed response can be traced back to changes in properties that underpin
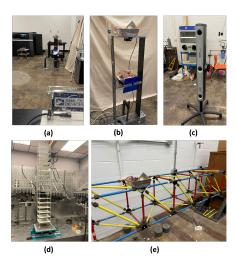
Figure 18: Experimental setup of studying the application of Platypus in Structural Health monitoring (SHM) for (a-b) studying building displacement compared with (c) Optotrak, and (d) earthquake response of multi-story buildings.

a structure's behavior and health. As a result, monitoring the response of a structure in various forms such as displacements, strains, and accelerations can provide important insights about structural behavior, health, and its operating conditions [10]. An extensive body of literature in the field of structural health monitoring thus focuses on correlating changes and anomalies in the monitored response with underlying damage [6, 47, 48] but their widespread adoption has been arguably hampered by the cost, power demand, and invasiveness of contact-based sensors.

Specifically, linear variable differential transformers (LVDT), linear potentiometers, and dial gauges require a reference point that typically is unavailable in complex environments such as bridges over waterways. While acceleration-based measurements are highly effective for dynamic vibration response, they do not directly measure displacements and require double integration rendering them inaccurate for measuring quasi-static displacement. Therefore, there is a technology gap to measure high-resolution micro-displacements in a non-invasive way over extended periods of time. Past efforts to address this gap mostly rely on GPS [14], laser vibrometry [22], fiber optics [47], or computer vision-based techniques [48], where either require large arrays of instrumentation with significant deployment costs, or does not provide the desired accuracy specially in long ranges, low visibility or NLoS conditions. There have also been a few cases of microwave radar technology applied to structural measurement applications using Synthetic Aperture Radar (SAR) [31] or active transponders [6, 12]. However, none of these techniques provide sub-mm displacement accuracy and are mainly evaluated in short-range lab experiments.

To demonstrate Platypus's application, we place two Platypus tags at two stories of a model building structure usually used to study the behavior of idealized mass-spring systems in structural dynamics instructions, shown in Figure 18. To measure the building displacements under horizontal forces, we manually applied a slow horizontal force at an estimated average speed of 8mm/sec on the top floor and compared the Platypus's estimated displacements
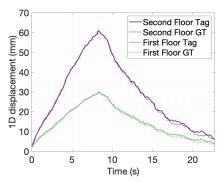

Figure 19: Platypus provides a similar performance compared to a $30k Optotrak system in estimating the micro-displacement of a two story model building structure, without the need for any active marker on the structure.

with an Optotrak Certus HD dynamic motion tracking system by National Digital Inc. The Optotrak uses four active optical markers attached at different parts of the specimen with a reported accuracy of 0.1mm. Figure 19 demonstrates the estimated displacements, achieving a promising median sub-mm accuracy.

6.1 Other Applications

Platypus provides sub-mm micro-displacement sensing with occlusion resistance even at extended ranges, which opens up many different applications in civil engineering, industrial robotics, or automation in industry 5.0 paradigm. In general, Platypus is expected to be applicable wherever visual markers or dedicated sensors are used for displacement tracking, with the added benefit of low-cost, ultra low-power and resilience to obstruction. Beyond structural health monitoring, some potential applications of Platypus include:

Industrial Robotics: Robotic systems require fine-grained situation awareness of the location and identity of surrounding objects to perform tasks such as grasping or assembly. Current visual systems struggle in the presence of obstructions or poor orientation that impedes direct-field-of-view [39]. Recent RF-based systems (e.g. RFID tags) aim to remedy this [25], yet operate over short distances (about ten meters). Platypus can enable an effective long-range object tracking solution that minimizes the amount of infrastructure needed to enable location-tracking in an industrial robotic context.

Predictive Maintenance for Industry 4.0: Machines in factories undergo significant micro-displacements that are a strong indicator of their overall health [35]. Tracking these displacements is challenging, especially those that occur within the interior of the machine or in locations obstructed from view. Platypus's ability to track micro-displacement overcomes this limitation to obtain a new cost-effective and scalable sensing modality to empower predictive maintenance in industry 4.0.

Sports Analytics: With the need for high mobility, long range, and high accuracy, tracking objects at high-speed in a sports stadium is challenging and typically requires complex visual sensing systems. Such systems traditionally use arrays of advanced cameras [19], primarily to enable line-of-sight access to the object being tracked. The long range and obstruction resilience of Platypus can

help augment such sensing systems, providing location-awareness when/where direct visual tracking fails.

7 DISCUSSION AND FUTURE WORK

Platypus still has several limitations including performance drops in fast displacements such as vibration. This is mainly due to Platypus's reliance to frequency-domain measurements that aggregates multiple chirps within a frame with the movements of the tag within a frame (10 ms) assumed negligible. As such, this paper purely focuses on pseudo-static micro-displacements which happen in millimeter-scale at long time periods without making any assumption on shape or direction of displacement. Nevertheless, Platypus is targeting a challenging problem that none of the existing methods (e.g. LDVT, or visual sensing) can practically solve. For our future work, we plan to take tag modulation inside a chirp thus improving the estimation rate from a few *ms* to *us*. This may increase power consumption by requiring a higher switching rate, but offers detection of both quasi-static and dynamic displacements.

In addition, the Van Atta array design used in Platypus's tag weighs approximately 0.1 kg and has overall dimensions of 8" x 1" x 1", so it is bulkier than traditional RFID tags [41, 45]. Therefore, if Platypus's tags were mounted on very delicate targets, the weight of the tags may affect the targets' motion. This paper mainly focuses on the signal processing algorithms needed to accomplish tracking. Nevertheless, in the primary application area of structural health monitoring, the weight and size of the tags are negligible compared to the buildings. In addition, given the millimeter-scale wavelength used, the tag and Van Atta structure can be miniaturized in future work to enable applications that require a more lightweight tracking system. To attach the tag to the structure, we envision using similar adhesives used for attaching strain gauges. In our future work, we plan to extend the synthetic reflector design for even longer ranges by adding a bi-directional amplifier in the transmission line.

8 RELATED WORK

Here we discuss works and topics related to Platypus.

8.1 RFID Tracking

Radio Frequency IDentification (RFID) is a widely used backscatter system to tag different objects and track them over time. It's been used for baggage tracking in airports [32], vehicle, people and animal tracking [9] and asset tracking in general. Depending on the application, RFID can measure small displacements of tagged objects with a much smaller form-factor and weight than the tags used in this paper. To achieve this, the fine phase changes of the RFID tag is monitored. [41] uses a multi-resolution sparse antenna array to track RFID tags on a centimeter level. [17, 18, 39, 43] uses phase to estimate tag orientation accurately. Processed phase can also be viewed as a time series for sensing activity types [7]. [8, 46] show that monitoring the phase helps in estimating parameters of periodic displacements such as vibration. [40, 45] uses phase measured across multiple antennas to create a high resolution hologram to track the position of tags to millimeter level.

However, all these systems make some assumptions in their problem definition which are not applicable in our use-case. They either assume a known displacement pattern (linear movements or periodic back and forth movements due to vibration) or static environments with one or handful tags moving with different speeds. In addition, RFID based systems suffer from small reading range (< 10 meters) and, therefore, all of these systems are tested in short ranges which effectively bound the noises due to multipath and background reflections. Our focus, however, is in monitoring sub-mm pseudo-static micro-displacements across 100s of meters reading range without any assumption on the targets of interest and their surrounding environment, or displacement patterns. Another key difference from RFID operation is the use of the tags and their modulation frequency as carrier waves to shift the micro-displacements to different frequency bins for simultaneously tracking the micro-displacement of multiple points, as opposed to RFID EPC Gen2 [11] which only provides phase measurements from a single tag at each time.

8.2 Radar-based Micro-Displacement Sensing

Radar interferometry for displacement sensing has been around for several decades [20, 21, 50]. These works custom design radar platforms to show proof of concept micro-displacement of a single object by monitoring the phase of reflected signals upon interferometry and unwrapping it. More recently, several works study the use of commodity mmWave radars and the natural reflections of the signal from the object surfaces for vibration detection [16], rotor orbit measurements [13], heart rate sensing [49], or hand writing detection [42]. Despite the achieved high accuracies, all these works rely on mmWave radars to estimate displacements purely based on the reflections from a single moving object or unique moving patterns (i.e. vibration, orbits, or chest movements due to heart activities) at short ranges, which is a conventional viewpoint of using radars for tracking. In contrary, Platypus leverages mmWave backscatter tags [24, 27, 29, 33], which are mainly designed for identification, localization and communication, to act as carriers of minute micro-displacements of multiple closely-located points amidst other moving objects.

9 CONCLUSION

This paper presents Platypus, a system that uses mmWave backscatter tags and commodity mmWave radars to perform sub-millimeter accurate displacement tracking. Uniquely, Platypus maintains this high accuracy at distances of over 100 meters and in situations where a line-of-sight path to the tag is unavailable. A detailed implementation and evaluation of Platypus demonstrates high accuracy, range and resilience to obstruction. We believe Platypus has direct applications to structural health monitoring, industrial robotics and automation. We leave a more exhaustive exploration of potential application domains of Platypus to future work.

of Illinois Urbana-Champaign for their helps in conducting in-field experiments.

REFERENCES

[1] 2020. Analog Devices SPDT Switch. https://www.analog.com/media/en/technical-documentation/data-sheets/ADRF5027.pdf.

[2] 2020. Analog Devices TinyRad. https://www.analog.com/media/en/technical-documentation/user-guides/ev-tinyrad24g-ug-1709.pdf.

[3] Mohammed Abdulkarem, Khairulmizam Samsudin, Fakhrul Zaman Rokhani, and Mohd Fadlee A Rasid. 2020. Wireless sensor network for structural health monitoring: a contemporary review of technologies, challenges, and future direction. *Structural Health Monitoring* 19, 3 (2020), 693–735.

[4] Kang Min Bae, Namjo Ahn, Yoon Chae, Parth Pathak, Sung-Min Sohn, and Song Min Kim. 2022. OmniScatter: extreme sensitivity mmWave backscattering using commodity FMCW radar. In *MobiSys*.

[5] Kshitiz Bansal, Manideep Dunna, Sanjeev Anthia Ganesh, Eamon Patamsing, and Dinesh Bharadia. 2022. R-fiducial: Reliable and Scalable Radar Fiducials for Smart mmwave Sensing. *arXiv preprint arXiv:2209.13109* (2022).

[6] Arthur Charléty, Eric Larose, Mathieu Le Breton, and Baillet. 2022. 2D Phase-based RFID localization for on-site landslide monitoring. (2022).

[7] Han Ding, Longfei Shangguan, Zheng Yang, Jinsong Han, Zimu Zhou, Panlong Yang, Wei Xi, and Jizhong Zhao. 2015. Femo: A platform for free-weight exercise monitoring with rfids. In *SenSys*.

[8] Chunhui Duan, Lei Yang, Qiongzheng Lin, and Yunhao Liu. 2018. Robust spinning sensing with dual-rfid-tags in noisy settings. *IEEE Transactions on Mobile Computing* (2018).

[9] Raymond E Floyd. 2015. RFID in animal-tracking applications. *IEEE Potentials* 34, 5 (2015), 32–33.

[10] B Glišic, Y Yao, S Tung, S Wagner, J Sturm, N Verma, Y Lee, D Blaauw, D Sylvester, J Gonzalez, et al. 2016. Structural Health Monitoring: Technological Advances to Practical Implementations. In *Proceedings of the IEEE 104*.

[11] GS1. 2022. EPC Radio-Frequency Identity Protocols Generation-2 UHF RFID Standard. "https://www.gs1.org/sites/default/files/docs/epc/gs1-epc-gen2v2-uhf-airinterface_i21_r_2018-09-04.pdf".

[12] Shanyue Guan, Jennifer A Rice, Changzhi Li, Yiran Li, and Guochao Wang. 2017. Structural displacement measurements using DC coupled radar with active transponder. *Structural Control and Health Monitoring* 24, 4 (2017), e1909.

[13] Junchen Guo, Meng Jin, Yuan He, Weiguo Wang, and Yunhao Liu. 2021. Dancing Waltz with Ghosts: Measuring Sub-mm-Level 2D Rotor Orbit with a Single mmWave Radar. In *IPSN*.

[14] et al Guzman-Acevedo. 2019. GPS, accelerometer, and smartphone fused smart sensor for SHM on real-scale bridges. *Advances in Civil Engineering* (2019).

[15] Gerhard Heinzel, Albrecht Rüdiger, and Roland Schilling. 2002. Spectrum and spectral density estimation by the Discrete Fourier transform (DFT). (2002).

[16] Chengkun Jiang, Junchen Guo, Yuan He, Meng Jin, Shuai Li, and Yunhao Liu. 2020. mmVib: micrometer-level vibration measurement with mmwave radar. In *MobiCom*.

[17] Chengkun Jiang, Yuan He, Xiaolong Zheng, and Yunhao Liu. 2018. Orientation-aware RFID tracking with centimeter-level accuracy. In *IPSN*. IEEE.

[18] Haojian Jin, Zhijian Yang, Swarun Kumar, and Jason I Hong. 2018. Towards wearable everyday body-frame tracking using passive RFIDs. *UbiComp* (2018).

[19] Paresh R Kamble, Avinash G Keskar, and Kishor M Bhurchandi. 2019. Ball tracking in sports: a survey. *Artificial Intelligence Review* 52, 3 (2019), 1655–1705.

[20] Seoktae Kim and Cam Nguyen. 2003. A displacement measurement technique using millimeter-wave interferometry. *IEEE Transactions on Microwave Theory and Techniques* 51, 6 (2003), 1724–1728.

[21] Seoktae Kim and Cam Nguyen. 2004. On the development of a multifunction millimeter-wave sensor for displacement sensing and low-velocity measurement. *IEEE Transactions on Microwave Theory and Techniques* 52, 11 (2004), 2503–2512.

[22] Bernd Köhler and James L Blackshire. 2006. Laser vibrometric study of plate waves for structural health monitoring (SHM). In *AIP Conference Proceedings*, Vol. 820. American Institute of Physics, 1672–1679.

[23] Orfeas Kypris and Andrew Markham. 2016. 3-D displacement measurement for structural health monitoring using low-frequency magnetic fields. *IEEE Sensors Journal* 17, 4 (2016), 1165–1174.

[24] Zhengxiong et. al. Li. 2019. FerroTag: a paper-based mmWave-scannable tagging infrastructure. In *SenSys*.

[25] Zhihong Luo, Qiping Zhang, Yunfei Ma, Manish Singh, and Fadel Adib. 2019. 3D backscatter localization for fine-grained robotics. In *NSDI*.

[26] Zhanxiong Ma, Jaemook Choi, Liu Yang, and Hoon Sohn. 2023. Structural displacement estimation using accelerometer and FMCW millimeter wave radar. *Mechanical Systems and Signal Processing* (2023).

[27] Mohammad Hossein Mazaheri, Alex Chen, and Omid Abari. 2021. mmTag: a millimeter wave backscatter network. In *SIGCOMM*.

[28] Ilya V Mikhelson and et al. 2011. Remote sensing of heart rate and patterns of respiration on a stationary subject using 94-GHz millimeter-wave interferometry. *IEEE Transactions on Biomedical Engineering* (2011).

[29] John Nolan, Kun Qian, and Xinyu Zhang. 2021. RoS: passive smart surface for roadside-to-vehicle communication. In *Proceedings of the 2021 ACM SIGCOMM 2021 Conference*. 165–178.

[30] Alan V. Oppenheim, Ronald W. Schafer, and John R. Buck. 1999. *Discrete-Time Signal Processing* (second ed.). Prentice-hall Englewood Cliffs.

[31] M Pieraccini, D Tarchi, H Rudolf, D Leva, G Luzi, G Bartoli, and C Atzeni. 2000. Structural static testing by interferometric synthetic radar. *Ndt & E International* 33, 8 (2000), 565–570.

[32] Longfei Shangguan, Zhenjiang Li, Zheng Yang, Mo Li, and Yunhao Liu. 2013. OTrack: Order tracking for luggage in mobile RFID systems. In *INFOCOM*.

[33] Elahe Soltanaghaei and et al. 2021. Millimetro: mmWave retro-reflective tags for accurate, long range localization. In *MobiCom*.

[34] Yi-Zhe Song and et al. 2014. Virtual visual sensors and their application in structural health monitoring. *Structural Health Monitoring* (2014).

[35] Toshihiro Takeshita and et al. 2011. Characteristics of a monolithically integrated micro-displacement sensor. In *IMEKO*.

[36] Lester Clare Van Atta. 1959. Electromagnetic reflector. US Patent 2,908,002.

[37] Chuyu Wang and et al. 2018. Multi-touch in the air: Device-free finger tracking and gesture recognition via cots rfid. In *INFOCOM*.

[38] Chuyu Wang and et al. 2021. Thru-the-wall Eavesdropping on Loudspeakers via RFID by Capturing Sub-mm Level Vibration. *UbiCOMP* (2021).

[39] Jue Wang and et al. 2013. RF-compass: Robot object manipulation using RFIDs. In *MobiCom*.

[40] Jingxian Wang and et al. 2019. Rfid tattoo: A wireless platform for speech recognition. *UbiCOMP* (2019).

[41] Jue Wang, Deepak Vasisht, and Dina Katabi. 2014. RF-IDraw: Virtual touch screen in the air using RF signals. *SIGCOMM* (2014).

[42] Teng Wei and Xinyu Zhang. 2015. mtrack: High-precision passive tracking using millimeter wave radios. In *MobiCom*. 117–129.

[43] Teng Wei and Xinyu Zhang. 2016. Gyro in the air: tracking 3d orientation of batteryless internet-of-things. In *MobiCom*.

[44] Binbin Xie and et al. 2020. Exploring commodity rfid for contactless sub-millimeter vibration sensing. In *SenSys*. 15–27.

[45] Lei Yang and et al. 2014. Tagoram: Real-time tracking of mobile RFID tags to high precision using COTS devices. In *MobiCom*.

[46] Lei Yang and et al. 2017. Tagbeat: Sensing mechanical vibration period with cots rfid systems. *IEEE/ACM transactions on networking* (2017).

[47] Fuzheng Zhang and et al. 2006. A Novel Micro-Displacement Sensor Based on Double Optical Fiber Probes Made through Photopolymer Materials. *Materials* (2006).

[48] Xinxiang Zhang, Yasha Zeinali, Brett A Story, and Dinesh Rajan. 2019. Measurement of three-dimensional structural displacement using a hybrid inertial vision-based system. *Sensors* 19, 19 (2019), 4083.

[49] Peijun Zhao and et al. 2020. Heart rate sensing with a robot mounted mmwave radar. In *ICRA*.

[50] Hongxing Zheng. 2005. A displacement and velocity measurement technique using millimeter-wave sensor. *journal of infrared and millimeter waves* (2005).